Indian Journal of Fibre & Textile Research
Vol. 49, December 2024, pp. 447-454
DOI: 10.56042/ijftr.v49i4.4462

Investigation of the contact resistance between stainless steel threads embedded in woven fabric

M Tokarska[a] & P Wróblewski

Lodz University of Technology, Faculty of Material Technologies and Textile Design,
Institute of Architecture of Textiles, 116 Zeromskiego St., 90-543 Lodz, Poland

Received 30 July 2023; revised received and accepted 26 December2023

This study investigates the contact resistance of stainless steel threads embedded in plain weave cotton fabric through weaving. The hybrid woven structures reflect the geometry of a woven fabric, the tension of the yarns in the structure, and the resulting pressure between them. Measurements of contact resistances of stainless steel threads are conducted. Four different cases of threads interlacing in the woven fabric are considered. Current-voltage characteristics and the temperature of the steel thread surface measurements are evaluated, determining the electric current threshold that avoids resistive heating. The four–electrode–four–wire method is employed for precise measurements. The uncertainty analysis is used to assess differences in the contact resistance measurements. The nonparametric Mann-Whitney U-Test compares contact resistances of steel threads in considered cases of interlacing. Results show that the contact resistance is lower for two threads interlaced in two directions compared to samples where a single thread occurs in one direction.

Keywords: Contact resistance, Interlacing configuration, Stainless steel thread, Uncertainty analysis, Woven fabric

1 Introduction

Electro-conductive textile materials gain significant attention due to their broad applications[1-6], particularly as sensors[7-11]. Textile-based sensors often operate by detecting changes in resistance[8,12]. The electro-conductive elements include linear textile materials (fibres, yarns) and flat textile products (woven, knitted, and non-woven fabrics). A conductive yarn can be integrated into a fabric by using traditional textile production methods such as weaving[13], knitting[11], and embroidery[14]. The inclusion of conductive metal or metal-coated yarns provides the foundation for creating sensing structures within textiles.

In woven fabrics, electro-conductive yarns intersect and overlap, forming electrical contact points at the junctions of warp and weft yarns. These contact points, whether single points, lines, or areas, contribute significantly to the electrical properties of the fabric. Based on Holm's theory[15], several factors determine the resistance of the electrical contact[11,16,17], such as the material used for each contact (yarn type and composition), the roughness of the contact surface (number of contact areas between yarns), the yarn contact area, and the mechanical pressure acting between electro-conductive yarns. Increased contact area and reduced surface roughness lower contact resistance, enhancing electrical conductivity. Conversely, high contact resistance can lead to hotspots, potentially causing discomfort or damage to fabric-based sensors and skin.[18,19]. Therefore, understanding and controlling contact resistance is crucial for the user's safety.

The contact between two components is modelled as an additional electrical resistance in a resistors network[20]. The woven structure, composed of two conducting components, strips and strip contacts, is studied from the point of view of the resistance effect of the components on woven structure electrical resistance[21]. It was shown that the contact resistance between conductive stips has a significant contribution to the resistance of the composite. The electrical resistance depends on the sample surface roughness[20,21]. The resistance of a woven fabric is related to the warp and weft directions[22,23]. The surface roughness causes the woven structure to exhibit electrical anisotropy[22-25].

The direct measurements of the contact resistance of two yarns do not reflect the geometry of a woven fabric[26]. The contact resistance is dependent on the tension of the yarns in the structure and the resulting pressure between them. The woven structures are designed in which conductive yarns are in mechanical

[a]Corresponding author.
E-mail: magdalena.tokarska@p.lodz.pl

and electrical contact with each other[27-29]. A hybrid woven fabric with stainless steel and polyester yarns was used to study the contact points, i.e. the overall contact electrical resistance in the specified points and the generated heat[28,29]. It was noticed that the weave pattern has a statistically significant influence on the contact resistance of yarns[28]. Moreover, researchers stated that yarns with a large diameter are recommended when a low contact resistance is desired. The contact resistance and the generated heat in the contact point were described in a mathematical model based on the behaviour of a metal oxide varistor[29].

Electro-conductive yarns embedded in textile structures create hybrid fabrics that are flexible, soft, and conformable. These hybrid textiles are widely used in wearable electronics (sensors, actuators, EMI shielding materials) or e-textile systems (electronic elements, circuits)[9,11,13,14,30]. A critical design parameter for such structures is the contact resistance between threads, which directly impacts their performance. This study aims to determine the contact resistance of stainless steel threads in different thread-weaving scenarios. To achieve this, steel threads are embedded into plain weave cotton fabric, replicating the actual geometry of a woven fabric, the tension of the yarns in the structure, and the resulting pressure between them.

2 Materials and Methods

2.1 Textile Samples

Tests were carried out using a 2-ply stainless steel thread (Fig. 1(a). The thread, made of SAE 316 L stainless steel, offers resistance to oxidation compared to silver, along with high strength and smoothness. It is flexible, resistant to bending, recyclable, has high thermal resistance and has good electrical conductivity. The thread is characterized by a linear mass of 500 tex and a twist of 170 turns/m. It has a low resistivity of 0.5 Ω/cm and is suitable for electronic components requiring an electric current below 50 mA according to the manufacturer's (Adafruit®) recommendations.

The fabric used is a plain weave cotton woven fabric (Fig. 1 (b)) with structural parameters: thickness - 0.899 mm, areal density - 228 g/m^2, bulk density - 254 kg/m^3, warp density – 12 yarns/cm, and weft density - 10 yarns/cm. Rectangular samples of4 cm × 10 cm were prepared by embedding stainless steel threads into the cotton fabric via weaving, enabling the exchange of at least one non-conductive yarn with a conductive thread. Four different thread interlacing configurations were considered (Table 1). For each configuration, two samples were prepared for testing, as outlined in Table 1.

2.2 Electrical Resistance

The electrical resistance of the conductive steel threads was measured based on standard EN 16812:2016[31]. The four-electrode – four-wire method was used due to the contact resistances R_{C1}, and R_{C2} between the electrodes and the sample being compensated. The test setup is shown in Fig. 2.

An electrical direct current was injected between two outer electrodes, and the voltage drop was recorded between two inner electrodes. The linear resistance of the thread was determined by linear regression using the following equation:

$$R(L) = a \cdot L + b \quad \ldots (1)$$

where L is the distance between voltage electrodes (edge to edge); $a = tg(\alpha)$, α, slope, and $b = R_{C1} + R_{C2}$. The linear resistance was calculated as:

$$R_L = a \quad \ldots (2)$$

The contact resistance at the interface between steel threads was measured using the test setups shown in Fig. 3 (variants I and II), as described in detail[21,28,29]. The applied electrical direct current was the same when determining the thread linear resistance.

Fig. 1 — Textile material (a) 2-ply stainless steel thread and (b) plain weave woven fabric

Table 1 — Different types of threads interlacing in woven fabric

Case	Description	Image
1×1	One steel thread in the horizontal direction and one in the vertical direction. (Sample 1, Sample 2)	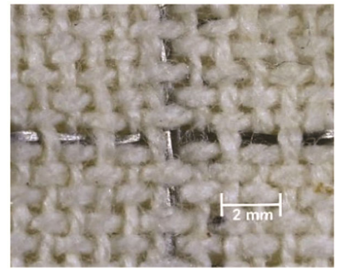
1×2	One steel thread in the horizontal direction and two in the vertical direction. (Sample 3, Sample 4)	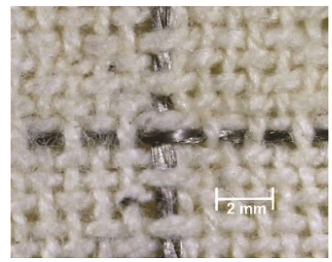
2×2	Two steel threads in both horizontal and vertical directions. (Sample 5, Sample 6)	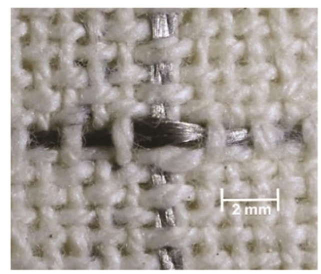
2×2*	Two adjacent steel threads in the horizontal direction in the repeat pattern and two in vertical direction. (Sample 7, Sample 8)	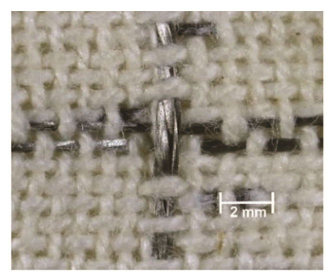

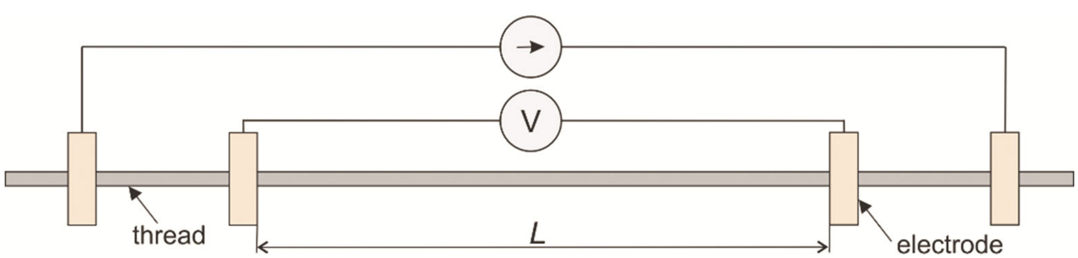

Fig. 2 — Four-electrode method for thread resistance measurement

The contact electrical resistance was calculated using the following formula:

$$R_C = \frac{V}{I} \quad \dots (3)$$

where *V* is the voltage drop; and *I,* the applied direct current.

A DC power supply (Agilent E3644A) was used as an ammeter with a resolution of 0.001 A, and a

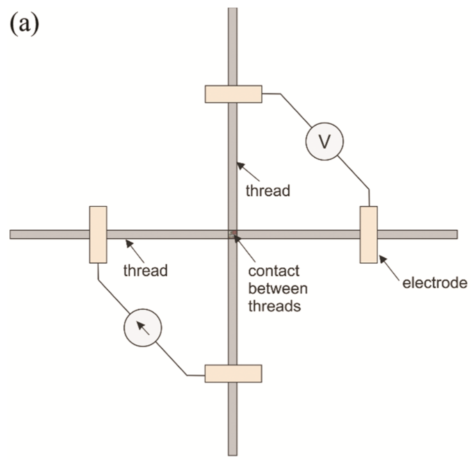

Fig. 3 — Four-electrode method for measuring the contact resistance between threads:(a) variant I and (b) variant II

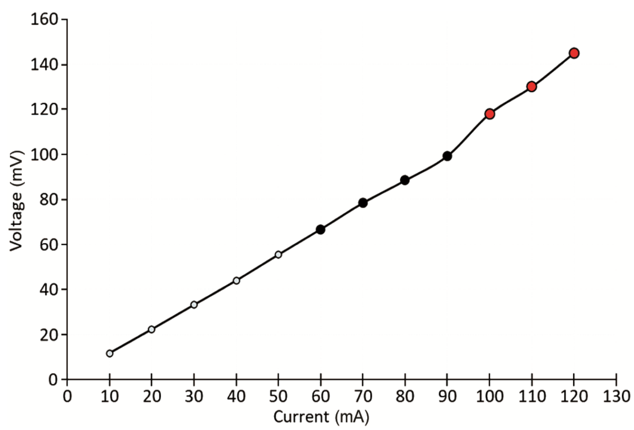

Fig. 4 — Current-voltage characteristic for steel thread

multimeter (Agilent 34410A) was used as a voltmeter with a resolution of 0.001 V. Four brass electrodes were used for voltage measurements.

2.3 Evaluation of Resistance Measurements

Evaluation of resistance measurements was conducted based on a guide to the expression of uncertainty in measurement[32]. The expanded uncertainty of output estimate *y* (a resistance) is used and expressed as follows:

$$U = k_p u_C(y) \quad \ldots (4)$$

Wherein

$$u_C^2(y) = \sum_{i=1}^{N} \left[\left(\frac{\partial f}{\partial x_i} \right)^2 \left(u_A{}^2(x_i) + u_B{}^2(x_i) \right) \right] \quad \ldots (5)$$

where k_p is the coverage factor (k_p=2 for the 0.95 confidence level); $u_C(y)$, combined standard uncertainty of *y*; *f*, functional relationship between output *y* (measurand) and input quantities x_i on which *y* depends; $\frac{\partial f}{\partial x_i}$, sensitivity coefficient; $u_A(x_i)$, Type A standard uncertainty; and $u_B(x_i)$, Type B standard uncertainty.

The Type A standard uncertainty is given as follows:

$$u_A(x_i) = \sqrt{\frac{\sum_{i=1}^{n_i} (x_{ik} - \overline{x}_i)^2}{n_i(n_i - 1)}} \quad \ldots (6)$$

where x_i are independent observations; n_i, number of repetitions; and x_i , the estimate of input quantity x_i.

The Type B standard uncertainty is evaluated by scientific judgment based on available information on the possible variability of an input quantity. Assuming a rectangular distribution of possible values, the Type B uncertainty can be determined from the following formula:

$$u_B(x_i) = \frac{d_e}{\sqrt{3}} \quad \ldots (7)$$

where d_e is the resolution of a measuring instrument.

The actual value of the measurement result estimated by *y* is in the interval [$y - U$, $y + U$] with a specified level of confidence, which means a coverage probability.

3 Results and Discussion

3.1 Electrical Characterization of the Steel Thread

All measurements are conducted at 24°C and 29 % relative humidity (RH). The current-voltage characteristic is determined with the distance between the voltage electrodes set at 7.0 cm. The current is applied up to 1.200 A. The voltage versus current curve is shown in Fig. 4.

Table 2 — Results of temperature measurements of steel thread surface

Parameter	Value	Image
Applied current	100 mA	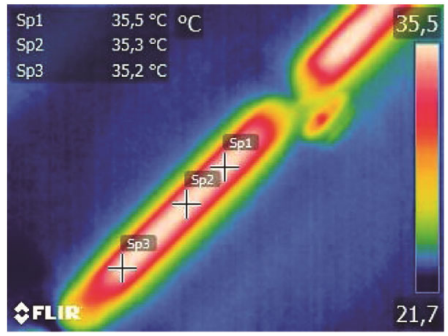
Temperature	35.3°C	
SD	0.2°C	
VC	0.4%	
Applied current	110 mA	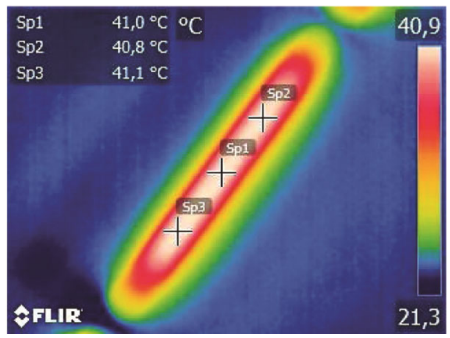
Temperature	41.0°C	
SD	0.2°C	
VC	0.4%	
Applied current	120 mA	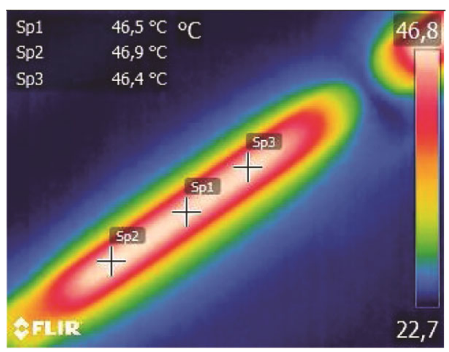
Temperature	46.6°C	
SD	0.3°C	
VC	0.6%	

SD - standard deviation, VC - variation coefficient

Voltage measurements remain stable to two significant digits for applied currents up to 90 mA, according to requirements of standard EN 16812:2016[31]. However, for currents in the range of 60-90 mA, the voltage measurements are not stable within three significant digits (black points in Fig. 4). Resistance heating of the thread is observed, and for currents of 100 mA or higher, unstable voltage measurements are recorded (red points in Fig. 4). Using a FLIR ThermaCAM E65 infrared camera, the temperature of the thread is measured before testing and for the last three current values, 100 mA, 110 mA, and 120 mA. Measurements are taken at three points on the thread surface. The mean values of the thread temperatures are shown in Table 2.

The initial mean thread temperature is 23.1°C (SD = 0.1°C, VC = 0.5%). The resistance heating of the steel thread is observed when excessive current is applied. The thread can be used safely when the current does not exceed 50 mA, as per the manufacturer's recommendation. This observation confirms that the thread behaviour follows Ohm's law for applied current up to 50 mA.

To test the linear electrical resistance of the steel thread, an applied current of 20 mA is used to avoid the heating effect. The distance between the voltage electrodes is in the range of 1.0 - 10.0 cm. The resulting resistance-distance characteristic ($R(L)$) is shown in Fig. 5.

The measurement results are approximated, yielding the following relationship:

$$R = 0.1376\,L + 0.1674 \quad \ldots (8)$$

wherein the coefficient of determination is 0.9996. Based on Eq. 8, the linear resistance of the steel thread is determined to be 0.14 Ω/cm, and the total contact resistance at electrodes is 0.17 Ω.

3.2 Contact Resistance between the Steel Threads

The contact resistance is measured in two variants: I and II (Fig. 3). The uncertainty budgets are summarized in Tables 3 and 4. A precision current source is used to set the electric current, and the Type A standard uncertainty for the electric current is equal to zero.The mean values of the contact resistance and the expanded uncertainty for tested samples are given in Table 5.

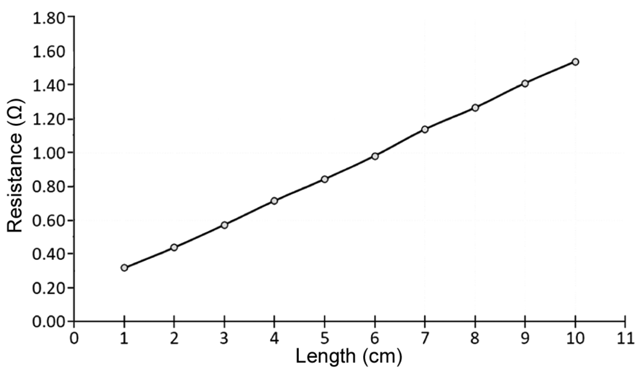

Fig. 5 — Resistance vs distance for steel thread

The uncertainty analysis confirms that the contact resistances obtained for the two variants (I and II) are comparable. The expanded uncertainty is a quantity defining an interval about the result of a measurement that may be expected to encompass a large fraction of the distribution of values that could reasonably be attributed to the measurand[32]. As a fraction, the coverage probability of 95 % is specified. The contact resistances and associated intervals are shown in Fig. 6. Each sample has two intervals due to two measuring variants (the couples of intervals). The interval obtained for variant I is located lower than the interval obtained for variant II for better readability.

Table 3 — Uncertainty budget for contact resistance measurement – Variant I

Sample	Electric current			Voltage				Combined standard uncertainty
	Estimate	Sensitivity coefficient	Type B standard uncertainty	Estimate	Sensitivity coefficient	Type A standard uncertainty	Type B standard uncertainty	
	A	V/A^2	A	V	1/A	V	V	Ω
1	0.020	$-1.59\cdot10^{3}$	$5.77\cdot10^{-4}$	0.636	50	$9.19\cdot10^{-3}$	$5.77\cdot10^{-4}$	1.03
2	0.020	$-1.42\cdot10^{3}$	$5.77\cdot10^{-4}$	0.570	50	$1.56\cdot10^{-2}$	$5.77\cdot10^{-4}$	1.14
3	0.020	$-1.45\cdot10^{3}$	$5.77\cdot10^{-4}$	0.580	50	$1.33\cdot10^{-2}$	$5.77\cdot10^{-4}$	1.07
4	0.020	$-1.51\cdot10^{3}$	$5.77\cdot10^{-4}$	0.603	50	$2.53\cdot10^{-2}$	$5.77\cdot10^{-4}$	1.53
5	0.020	$-9.75\cdot10^{2}$	$5.77\cdot10^{-4}$	0.390	50	$2.19\cdot10^{-2}$	$5.77\cdot10^{-4}$	1.23
6	0.020	$-1.11\cdot10^{3}$	$5.77\cdot10^{-4}$	0.445	50	$1.56\cdot10^{-2}$	$5.77\cdot10^{-4}$	1.01
7	0.020	$-9.98\cdot10^{2}$	$5.77\cdot10^{-4}$	0.399	50	$2.04\cdot10^{-2}$	$5.77\cdot10^{-4}$	1.17
8	0.020	$-1.09\cdot10^{3}$	$5.77\cdot10^{-4}$	0.436	50	$1.19\cdot10^{-2}$	$5.77\cdot10^{-4}$	0.87

Table 4 — Uncertainty budget for contact resistance measurement – Variant II

Sample	Electric current			Voltage				Combined standard uncertainty
	Estimate	Sensitivity coefficient	Type B standard uncertainty	Estimate	Sensitivity coefficient	Type A standard uncertainty	Type B standard uncertainty	
	A	V/A^2	A	V	A	V/A^2	A	Ω
1	0.020	$-1.44\cdot10^{3}$	$5.77\cdot10^{-4}$	0.575	50	$9.56\cdot10^{-3}$	$5.77\cdot10^{-4}$	0.96
2	0.020	$-1.39\cdot10^{3}$	$5.77\cdot10^{-4}$	0.556	50	$1.37\cdot10^{-2}$	$5.77\cdot10^{-4}$	1.06
3	0.020	$-1.58\cdot10^{3}$	$5.77\cdot10^{-4}$	0.630	50	$9.09\cdot10^{-3}$	$5.77\cdot10^{-4}$	1.02
4	0.020	$-1.58\cdot10^{3}$	$5.77\cdot10^{-4}$	0.630	50	$1.87\cdot10^{-2}$	$5.77\cdot10^{-4}$	1.31
5	0.020	$-9.61\cdot10^{2}$	$5.77\cdot10^{-4}$	0.384	50	$2.15\cdot10^{-2}$	$5.77\cdot10^{-4}$	1.21
6	0.020	$-1.04\cdot10^{3}$	$5.77\cdot10^{-4}$	0.415	50	$2.88\cdot10^{-2}$	$5.77\cdot10^{-4}$	1.56
7	0.020	$-9.84\cdot10^{2}$	$5.77\cdot10^{-4}$	0.394	50	$1.42\cdot10^{-2}$	$5.77\cdot10^{-4}$	0.91
8	0.020	$-1.07\cdot10^{3}$	$5.77\cdot10^{-4}$	0.427	50	$1.63\cdot10^{-2}$	$5.77\cdot10^{-4}$	1.02

The mean values of the contact resistance and the expanded uncertainty for tested samples are given in Table 5.

Table 5 — Results of contact resistances of steel threads embedded in woven fabric

Sample	Variant I		Variant II	
	Contact resistance, Ω	Expanded uncertainty, Ω	Contact resistance, Ω	Expanded uncertainty, Ω
1	31.78	2.05	28.74	1.92
2	28.48	2.27	27.78	2.11
3	28.99	2.14	31.50	2.03
4	30.13	3.07	31.51	2.61
5	19.49	2.47	19.22	2.42
6	22.27	2.03	20.76	3.12
7	19.96	2.34	19.68	1.82
8	21.82	1.73	21.33	2.04

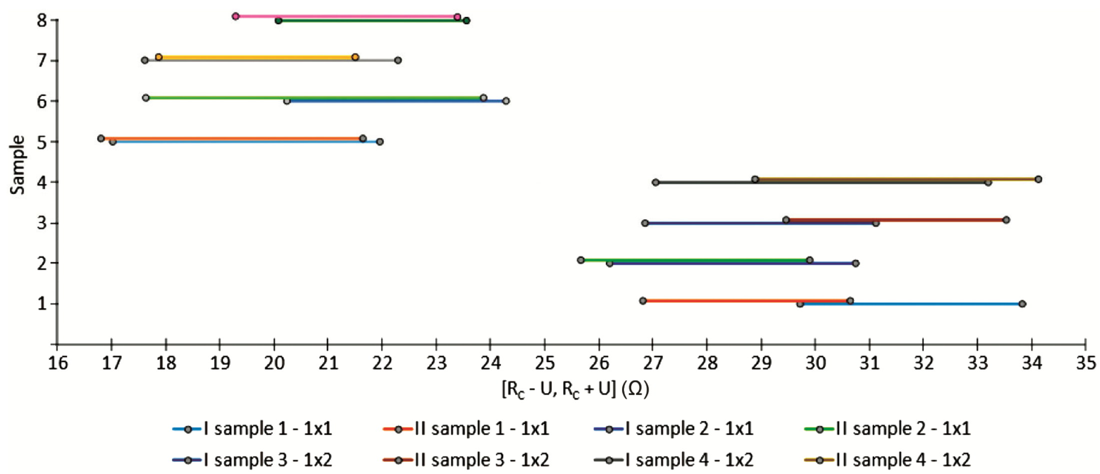

Fig. 6 — Contact resistances of steel threads with associated intervals

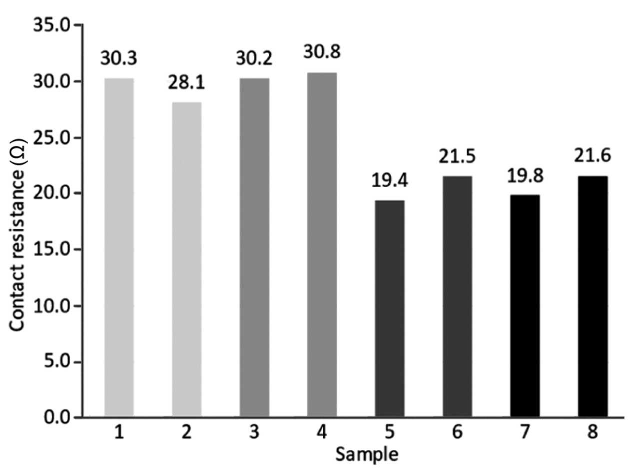

Fig. 7 — Average value of contact resistance for threads embedded in woven fabric

Partially left-overlapped intervals are observed for samples 1, 2, 5, 6, and 8, while partially right-overlapped intervals are noted for samples 3 and 4. For sample 7, the intervals are completely overlapped. This indicates that the contact resistance measurement from the two variants yields comparable results. The selection of adjacent threads for current electrode connections (Fig. 3) does not affect the accuracy of the contact resistance measurement. The average value of the contact resistance for all samples is shown in Fig. 7.

A significance test for the influence of the cases described in Table 1 on contact resistance measurements is performed using the nonparametric Mann-Whitney U-Test[33] with a significance level of $\alpha = 0.05$ (Table 6). The Statistica® program is used. The value associated with the null hypothesis states that there are no significant differences between the groups and denotes the probability of rejecting the null hypothesis when it is true.

The statistical analysis indicates that the contact electrical resistances of embedded threads, as described in cases 1×1 or 1×2, do not differ significantly ($p>\alpha$, $p=0.6985$). Similarly, threads embedded in cases 2×2 or 2×2*yield comparable results. Significant differences in contact resistance ($p<\alpha$, $p=0.0303$) are observed only when two threads in both directions (weft and warp) participate in the interlacing (case 2×2 or 2×2*), resulting in a lower contact resistance compared to cases 1×1 or 1×2.

Table 6 — Statistical analysis

Compared cases		p-value
1×1 (samples 1 and 2)	1×2 (samples 3 and 4)	0.6985
2×2 (samples 5 and 6)	2×2* (samples 7 and 8)	0.6985
1×1 and 1×2	2×2 and 2×2*	0.0303

4 Conclusion

The electrical characterization of steel threads embedded in woven fabric reveals significant insights into their resistive behaviour under varying current conditions. The main findings of this work are as follows.

a) The current-voltage characteristics and surface temperature measurements of the steel thread allow for the determination of the electric current range in which resistance heating of the sample is not observed.
b) Significant differences in contact resistance are observed (at 0.05 level of significance) depending on the interlacing configuration of the threads in the woven fabric. The contact resistance is lower when two threads are interlaced in two directions (weft and warp) compared to when only one thread is used in one direction.
c) The uncertainty analysis conducted enables an assessment of the contact resistance measurements for different electric scheme variants. The analysis confirms that both variants yield comparable results with a 95 % coverage probability.

References

1 Shabani A, Hylli M & Kazani I, *Tekstilec*, 65 (2022) 194.
2 Li-Chuan J, Xian-Xiang J, Wen-Jin S, Yun-Peng Z, Ling X, Ding-Xiang Y, Hai-Jun S & Zhong-Ming L, *ACS Appl Mater Interf*, 12 (2020) 53230.
3 Leśnikowski J, *J Text Inst*, 111 (2020) 604.
4 Song J, Zhang Y, Yang Y, Liu H, Zhou T, Zhang K, Li F, Xu Z, Liu Q & Li J, *Biomed Eng*, 19 (2020) 1.
5 Ankhili A, Tao X, Cochrane C, Coulon D & Koncar V, *Materials*, 11 (2018) 1.
6 Gil I, Fernández-García R & Tornero J A, *Text Res J*, 89 (2019) 1573.
7 Biermaier C, Bechtold T & Pham T, *Sensors*, 21 (2021) 1.
8 Husain M D, Kennon R & Dias T, *J Ind Text*, 44 (2014) 398.
9 Capineri L, *Procedia Eng*, 87 (2014) 724.
10 Han W, Wu Y, Gong H, Liu L, Yan J, Li M, Long Y & Shen G, *Nano Res*, 14 (2021) 2810.
11 Atalay O & Kennon W R, *Sensors*, 14 (2014) 4712.
12 Zhang X & Ma P, *Autex Res J*, 18 (2018) 181.
13 Zysset C, Kinkeldei T, Münzenrieder N, Petti L, Salvatore G & Tröster G, *Text Res J*, 83 (2013) 1130.
14 Kannaian T, Neelaveni R & Thilagavathi G, *J Ind Text*, 42 (2013) 303.
15 Holm R, *Electric contacts, Theory and applications* (Springer, Verlag Berlin Heidelberg) 1967.
16 Mitschang P, Rudolf R & Neitzel M, *J Thermoplast Compos Mater*, 15 (2002) 127.
17 Zafar H, Vučinić-Vasić M, Popović Ž, Babković K & Stojanović G M, *J Ind Text*, 53 (2023) 1.
18 Balakatounis K C & Angoules A G, *Eplasty*, 8 (2008) 283.
19 Banaszczyk J, Schwarz A, De-Mey G & Van-Langenhove L, *J Appl Polym Sci*, 117 (2010) 2553.
20 Pantoja J J, Cristancho J, Rodriguez J, Rivera C, Román F, Vega F, Kasmi C & Al-Yafei F, *Proceedings*, URSI GASS (Rome, Italy), (2020).
21 Tokarska M, *Materials*, 15 (2022) 1.
22 Tokarska M & Gniotek K, *J Text Inst*, 106 (2015) 9.
23 Tokarska M, *J Electron Mater*, 46 (2017) 1497.
24 Kazani I, De-Mey G, Hertleer C, Banaszczyk J, Schwarz A, Guxho G & Van-Langenhove L, *Text Res J*, 81 (2011) 2117.
25 Tyurin I N, Getmantseva V V & Andreeva E G, *Fibre Chem*, 51 (2019) 139.
26 Dhawan A, Seyam A M, Ghosh T K & Muth J F, *Text Res J*, 74 (2004) 913.
27 Gunnarsson E, Karlsteen M, Berglin L & Stray J, *Text Res J*, 85 (2015) 499.
28 Vasile S, Deruck F, Hertleer C, De-Raeve A, Ellegiers T & De-Mey G, *Autex Res J*, 17 (2017) 170.
29 Hertleer C, Meul J, De-Mey G, Vasile S, Odhiambo S A & Van-Langenhove L, *Autex Res J*, 20 (2020) 133.
30 Chatterjee K, Tabor J & Ghosh T K, *Fibers*, 7 (2019) 1.
31 EN 16812:2016. Textiles and textile products—Electrically conductive textiles—Determination of the linear resistance of conductive tracks.
32 ISO/IEC Guide 98-3:2008. Uncertainty of Measurement—Part 3: Guide to the Expression of Uncertainty in Measurement (GUM:1995).
33 Corder G W & Foreman D I, *Nonparametric statistics for non-statisticians: A step-by-step approach* (Wiley, Hoboken) 2009.